Numerical implementation of a inverse scattering problem in 3D

A PROJECT REPORT

by

Meesala Raviteja

Tata Institute of Fundamental Research

Centre for Applicable Mathematics

Bangalore – 560 065

AUGUST 2017

Contents

List of Figures

Chapter 1

Introduction

The focus of this project has been to implement a inverse scattering reconstruction algorithm as proposed in [1]. A number of examples were tried out to test the working of the algorithm. Since the input required for the inverse problem is the far-field data, this is generated by solving the direct problem first.

This report is organized as follows. Chapter 2 deals with the direct problem and the numerical techniques involved in solving it. Further, the generation of far-field data from the scaterred field is described. Chapter 3 details about the inverse problem and reconstruction algorithm used. The simulations performed and the results obtained are detailed in Chapter 4 and Chapter 5.

Chapter 2

Direct Problem

Consider the scattering of a time harmonic acoutic wave by an obstacle D $\subset \mathbb{R}^3$. The governing equations are as follows:

$$\Delta u + k^2 = 0, \text{ in } \mathbb{R}^3 \backslash D \tag{2.1}$$

$$u = u^i + u^s \tag{2.2}$$

$$\lim_{r\to\infty} r(\frac{\partial u^s}{\partial r} - iku^s) \tag{2.3}$$

$$u = v, \text{ on } \partial D; \tag{2.4}$$

$$\frac{1}{\rho}\frac{\partial u}{\partial \nu} = \frac{1}{\rho_D}\frac{\partial v}{\partial \nu} \tag{2.5}$$

where u^i is the incident wave, u^s is the resultant scattered field. Direct scattering problems are concerned with finding the solutions of the helmholtz's equation in an exterior domain. Even though the helmholtz equation is elliptic, finite element methods and finite difference methods are not easily applicable. The solution is required to satisfy the sommerfield condition at infinity and imposing this poses a difficulty with these methods. This is avoided while using the Integral equation methods. The resulting intergral equations are solved only on the boundary and can be seen to verify the radiation condition automatically. A detailed description of the following boundary element formulation, used to solve the direct problem can be found at [2].

2.1 BIE Formulation

The following equation can be derived from the green's representation formula:

$$u(x) = u^i(x) - \int_{\partial D} g(x,y)\frac{\partial u}{\partial \nu}(y)dy \tag{2.6}$$

As can be seen, with the knowledge of the normal derivative $\frac{\partial u}{\partial \nu}$ on the boundary, one can obtain u. Here $g(x,y)$ is the acoustic green's function given by:

$$g(x,y) := \frac{e^{ik|x-y|}}{4\pi|x-y|} \tag{2.7}$$

The normal derivative can be estimated by solving the following boundary integral equation:

$$\frac{1}{2}u_\nu(x) + \int_{\partial D} \frac{\partial \Phi(x,y)}{\partial \nu(y)} u_\nu(x)ds(y) - i\eta \int_{\partial D} \Phi(x,y)u_\nu(x)ds(y) = \frac{\partial u^i}{\partial \nu}(x) - i\eta u^i(x); x \in \partial D \tag{2.8}$$

where Φ is a test function.

2.2 Far Field data

The far-field data required for solving the inverse problem is computed as follows:

$$u_\infty(\hat{x}) = -\frac{1}{4\pi}\int_{\partial D} \frac{\partial u}{\partial \nu}(y)e^{-k\hat{x}.y}ds(y), \hat{x} \in \omega \tag{2.9}$$

Chapter 3

Inverse Problem

The inverse problem that is explored in this work concerns with the estimation of the obtstacle boundary D. This is estimated from the knowledge of $u_\infty(\hat{x}$,d), the far-field data as indicated in the previous chapter, for $\hat{x}$ and d on the unit sphere $\Omega := \{\ x : |x| = 1\}$. The entire far-field data is obtained fixing the wavenumber k and is obtained for plane waves varying in direction d.

Several numerical apporaches have been studied for this problem. Some techniques such as [3] [4] [4] have been based on nonlinear optimization techniques. However, these methods seldom seem to be used in practical applications of shape reconstruction problems as they require certain infromation related to the geometry of the obstacles. The sampling method technique explored in this work was first developed by colton and Kirsch [6]. The strength of this method lies on the fact that it doesnot require any apriori information related to the boundary conditions satisfied by the field on the boundary of the scatterer.

3.1 The sampling method

The following results are fundamental to the development of the sampling method. Suppose for some $z \in D$, we can find a g = g(.,z) from the far-field equation:

$$\int_\Omega u_\infty(\hat{x}, d) g(d, z) ds(d) = e^{ik\hat{x}\cdot z} \tag{3.1}$$

Using Rellich's lemma [7], the following is established:

$$\int_{\Omega} u_s(\hat{x}, d) g(d, z) ds(d) = \frac{e^{ik|x-z|}}{|x-z|} \tag{3.2}$$

Further, basing on the boundary conditions satisfied by u in addition to the above conditions, it is expected that $g(., z)$ becomes "unbounded" as z approaches ∂D. Hence, inorder to estimate ∂D one must detect $g(., z)$ for z where it becomes "large". A detailed description of the method and its variants can be studied at [1].

3.2 The numerical method

The numerical technique used is to approximate both u_∞ and $g(d, \cdot)$ using their values for n different plane waves (d), that are probed at those same n locations ($\hat{x}$). These directions are generated by considering the normals from the triangulated surface of a unit sphere.
Let $\Psi_j(\hat{x})$ denote the basis function for the space of continuous piecewise linear elements. Then

$$g(\hat{x}, z) = \sum_{j=1}^{n} g(\hat{x_j}, z) * \Psi_j(\hat{x}) \tag{3.3}$$

u_∞ is approximated similarly. The discretized integral equation that is solved to estimate $g(\cdot, z)$ is as follows:

$$\int_{\Omega_h} [\sum_{l=1}^{n} u_\infty(\hat{x_j}, \hat{x_l}) \Psi_l(\hat{x})][\sum_{i=1}^{n} g(\hat{x_i}, z) \Psi_i(\hat{x})] ds = e^{ik\hat{x_j} \cdot z} \tag{3.4}$$

This results in a system of linear equations with unknowns $g(x_j, z)$ for j ranging from 1 to n. Taking an l^2 norm of the solution gives an estimate for $\|g(\cdot, z)\|$.

Chapter 4

Experimental Setup

A set of experiments are performed over 4 types of obstacles placed at the origin.

1. Sphere
2. Two spheres
3. Ellipse (a skewed convex shape)
4. Smooth-plus-sign (a non convex shape)

Initally the simulations are performed to generate the far field data by solving for the exterior dirichlet problem. The tools utilized for this are as follows:

1. bempp (A python package to solve the direct problem and generate far-field data) [8]
2. gmsh (To generate mesh over obstacles and generate unit normals over a sphere) [9]
3. Octave/Matlab (For implementing the inverse problem) [11]
4. Paraview (To visualize the resulting images) [10]

4.1 Routines developed

The inverse problem is now solved using the far-field data generated as in the previous step. The following (key)routines were developed for the inverse problem to compute using Octave.

1. main.m : The main file that calls other routines
2. Assembling_A.m : Assembles the matrix
3. getimage.m, visualize.m : Calculates norm(g) and generates the vtk file

4.2 Parameters used

1. Wavenumber k := 10, for all simulations
2. The number of unit normals used on the sphere: 108/258 (generated through gmsh)

4.3 Verification

The accuracy of the solution to the direct problem could be verified by plotting u around the obstacle. For the inverse problem, using the visualization tool Paraview, the value g is plotted around the object enclosed in a cubic volume. This data is visualized through 3 slices (planes in x, y, z direction) made at the origin.

Chapter 5

Results

5.1 Example 1: Unit Sphere

5.1.1 Solution to Direct problem

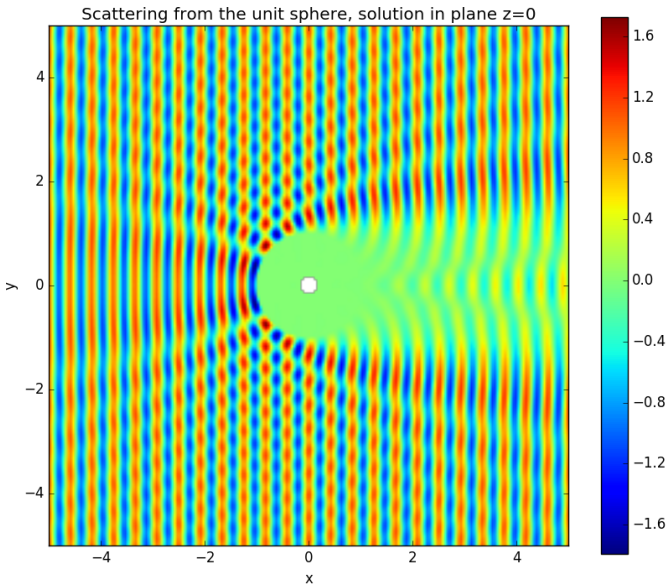

Figure 5.1: Plot of u when scattered with a plane wave along x-axis

5.1.2 Reconstruction using far-field data

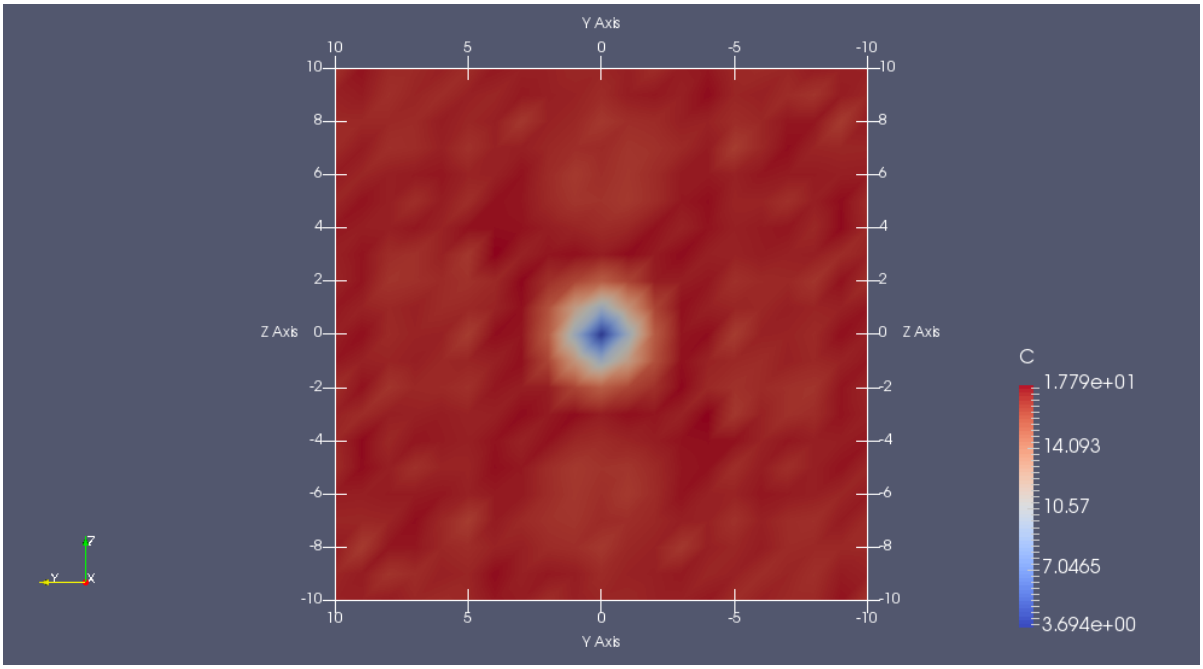

Figure 5.2: Slice along x-axis for a Unit-sphere

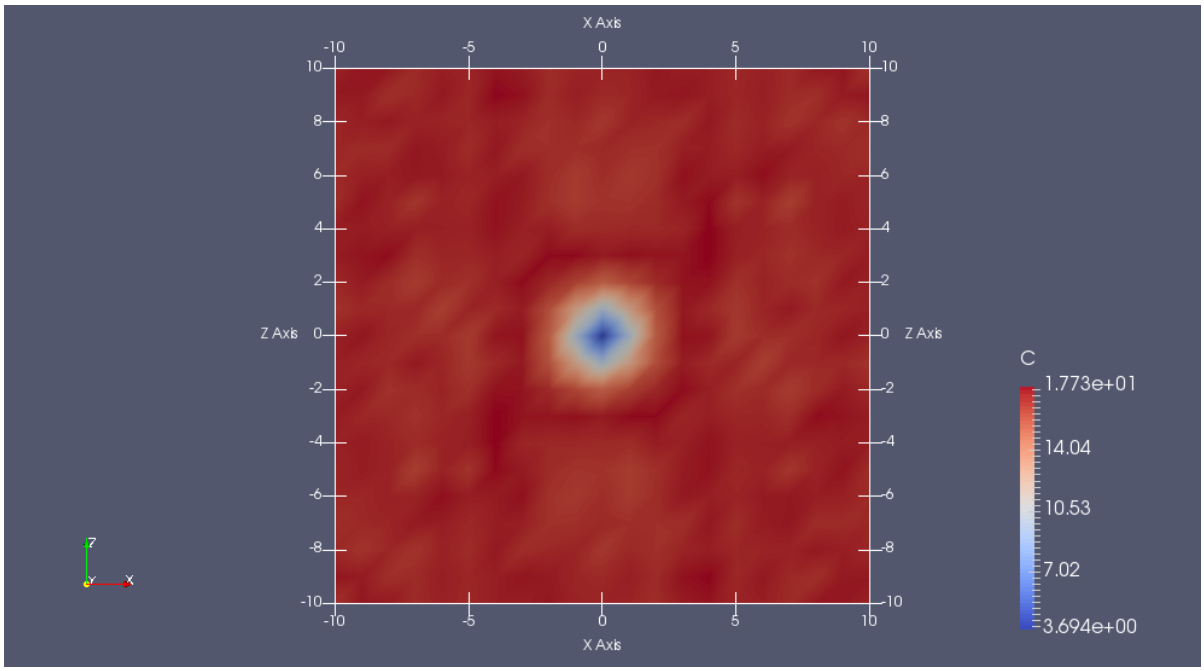

Figure 5.3: Slice along y-axis for a Unit-sphere

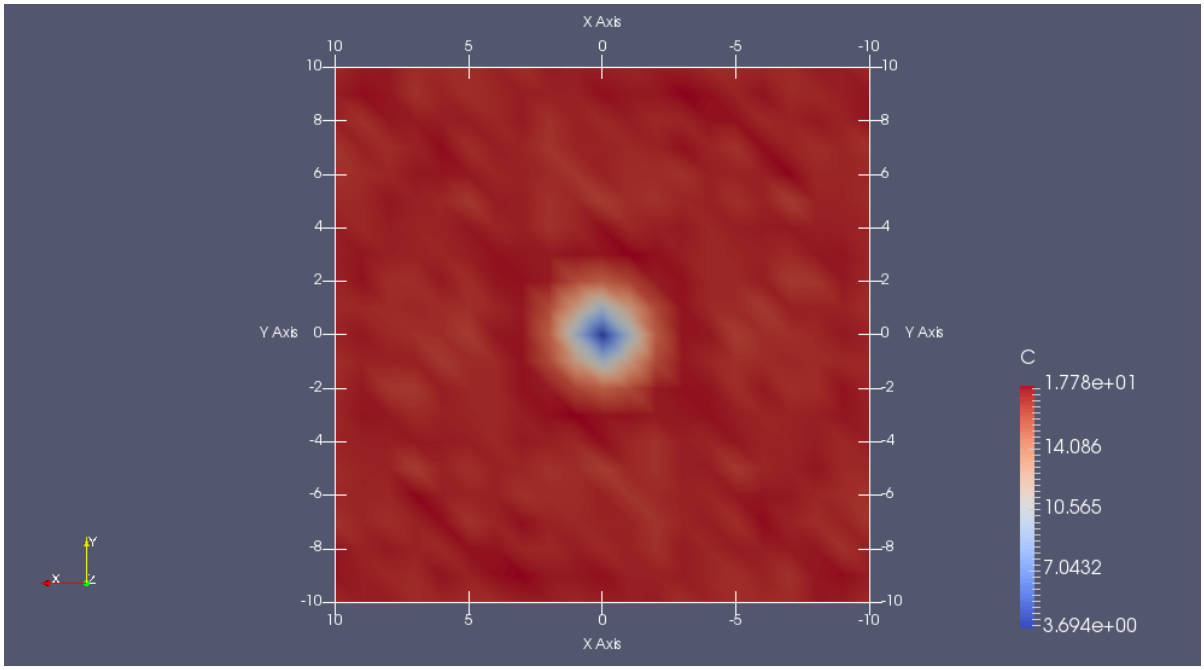

Figure 5.4: Slice along z-axis for a Unit-sphere

5.2 Example 2: Two Spheres

5.2.1 Mesh of Two Spheres

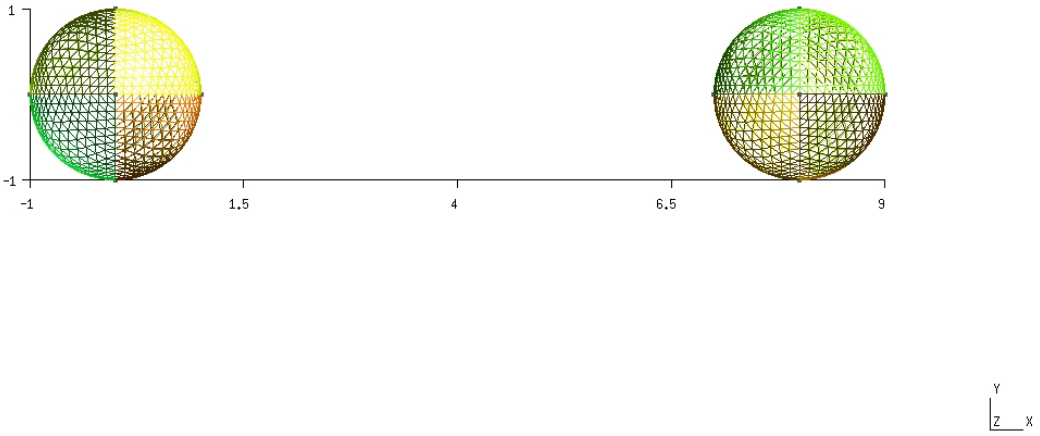

Figure 5.5: Two spheres mesh

5.2.2 Reconstruction using far field data

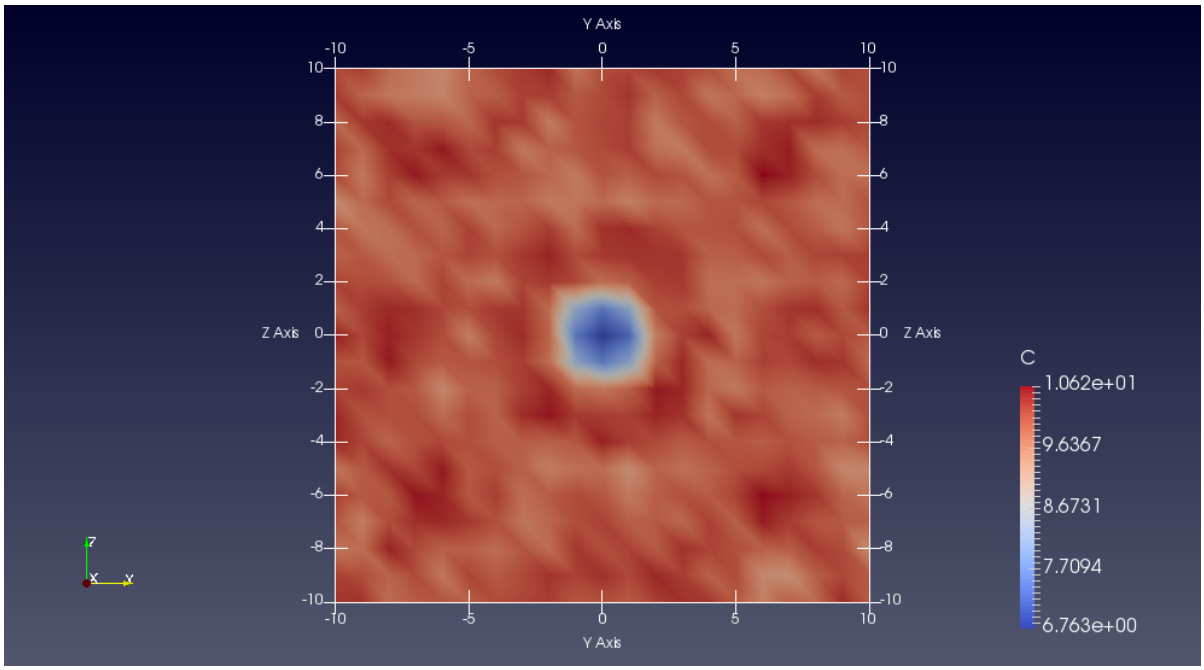

Figure 5.6: Slice along x-axis with two-spheres

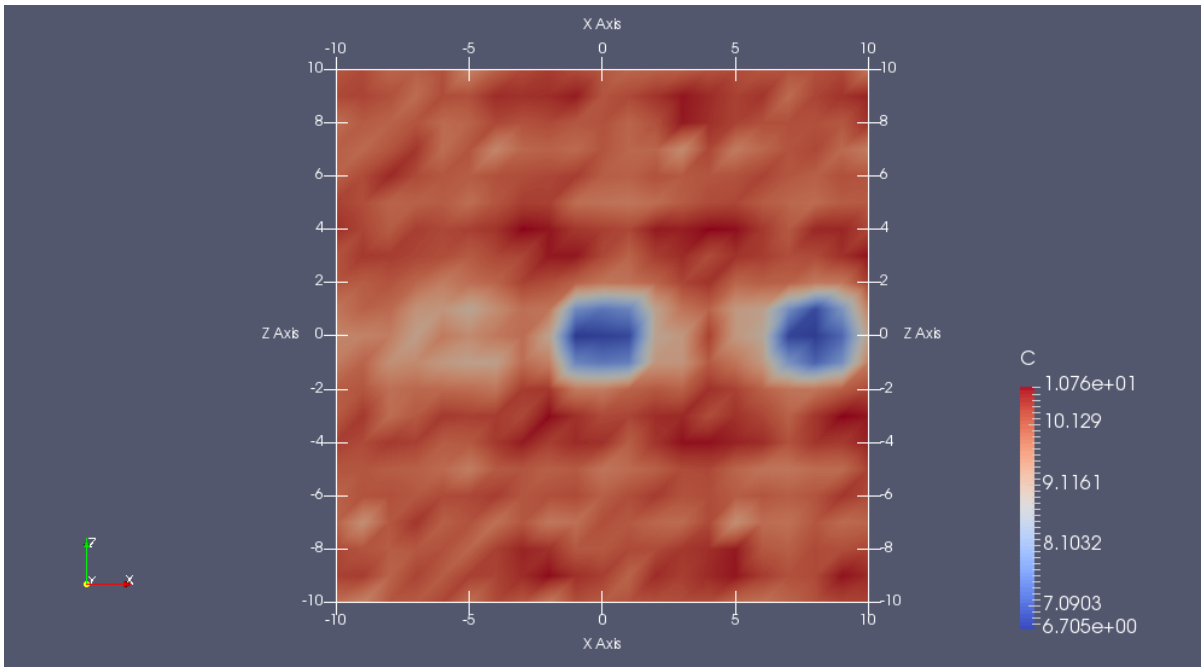

Figure 5.7: Slice along y-axis with two-spheres

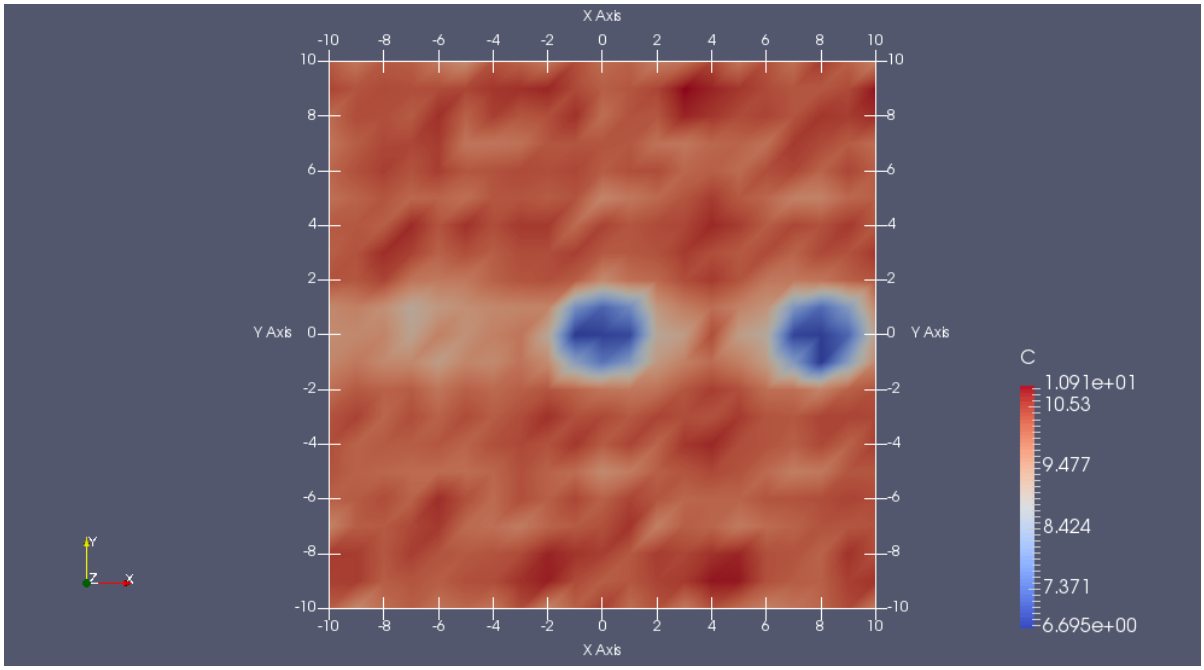

Figure 5.8: Slice along z-axis with two-spheres

5.3 Example 3: Ellipse

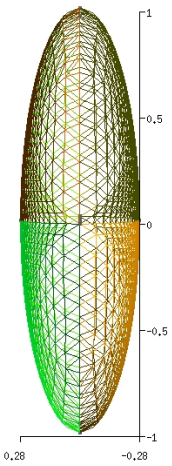

(a) Mesh of ellipse along x-axis

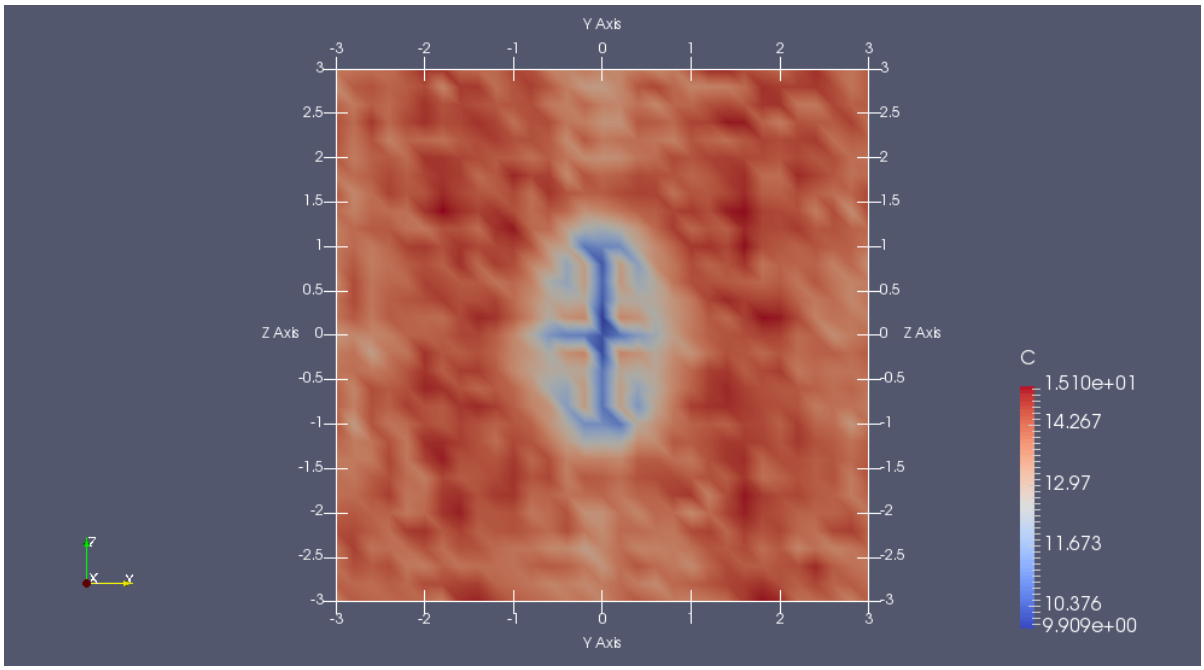

(b) Reconstructed ellipse along x-axis

Figure 5.9: Ellipse along x-axis

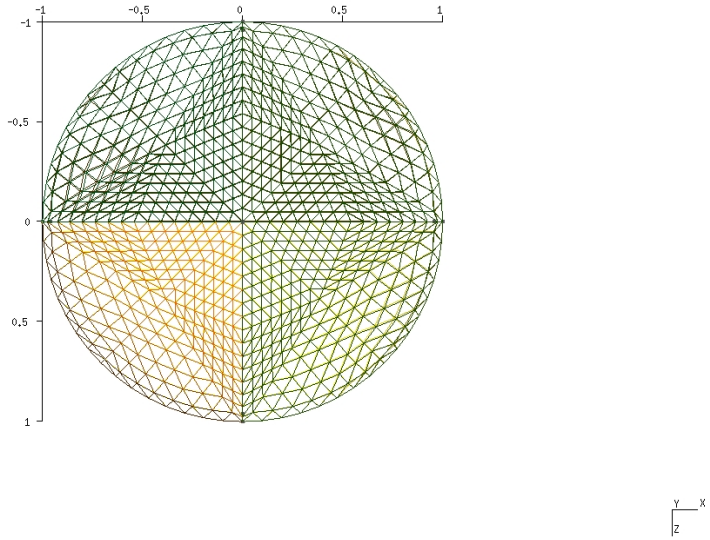

(a) Mesh of ellipse along x-axis

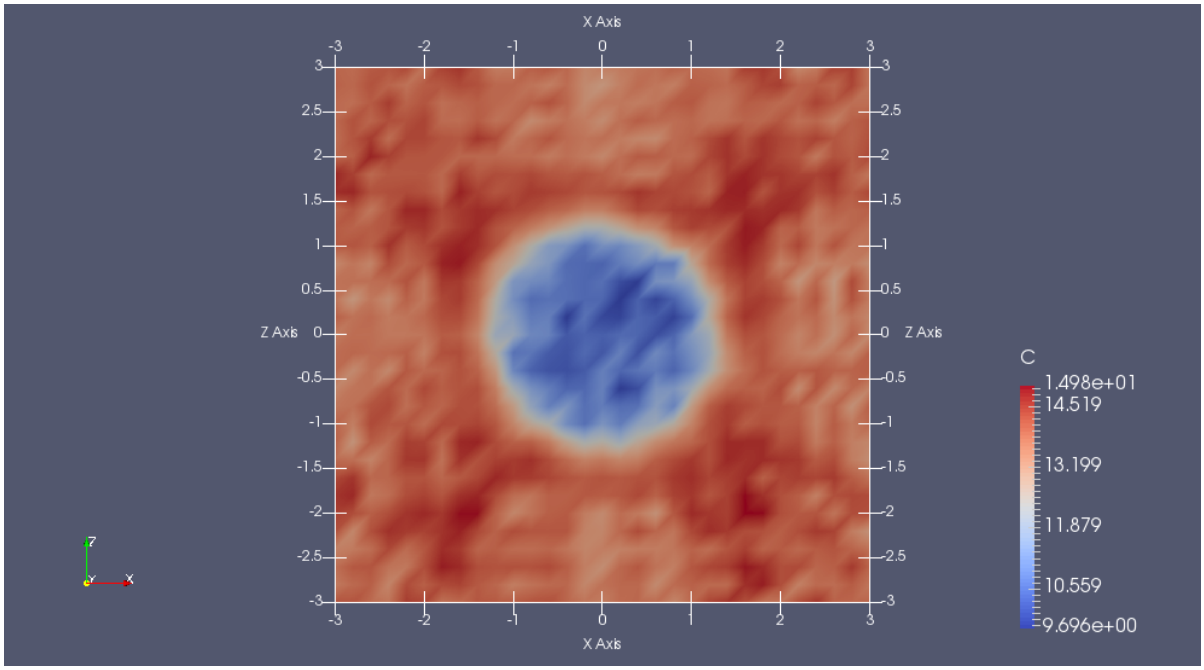

(b) Reconstructed ellipse along x-axis

Figure 5.10: Ellipse along y-axis

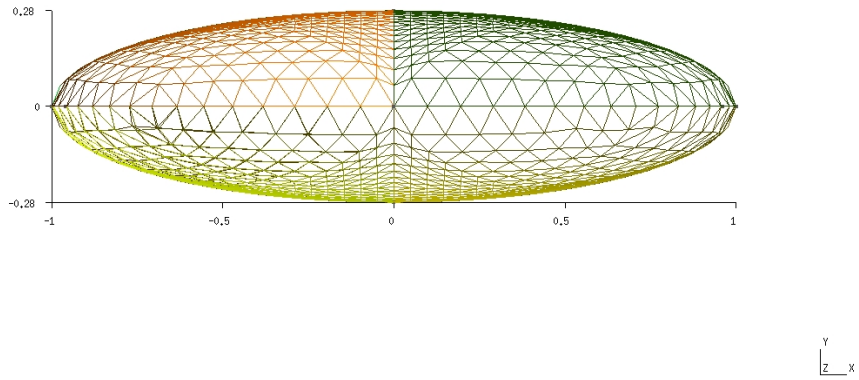

(a) Mesh of ellipse along z-axis

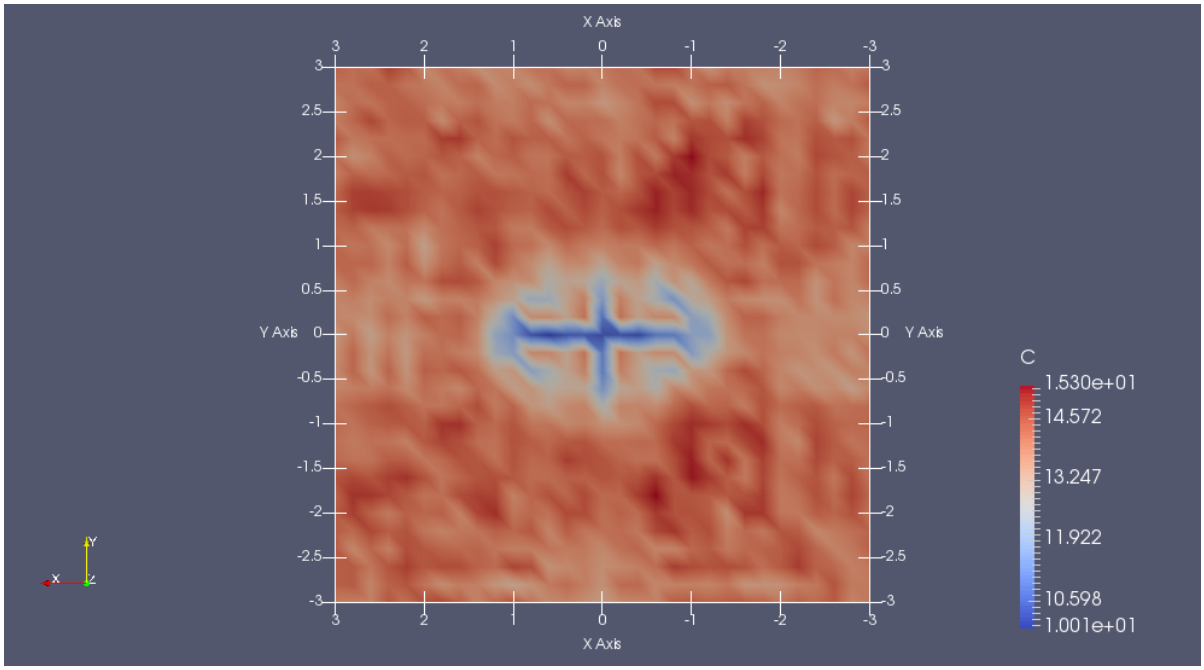

(b) Reconstructed ellipse along z-axis

Figure 5.11: Ellipse along z-axis

5.4 Example 4: Star

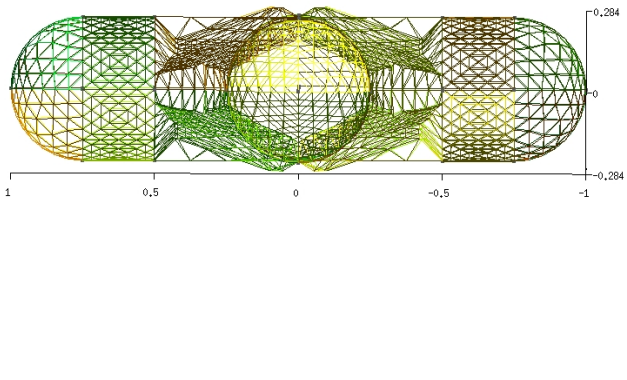

(a) Mesh of Star along x-axis

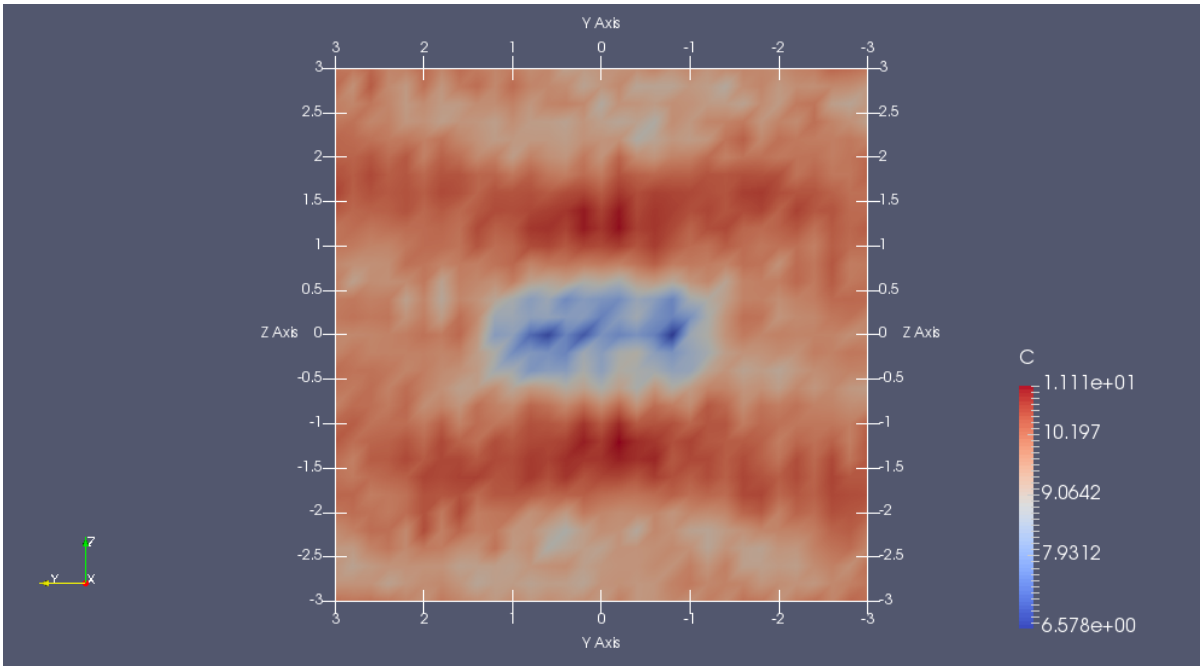

(b) Reconstructed Star along x-axis

Figure 5.12: Star along x-axis

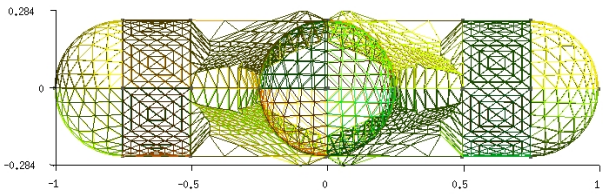

(a) Mesh of Star along y-axis

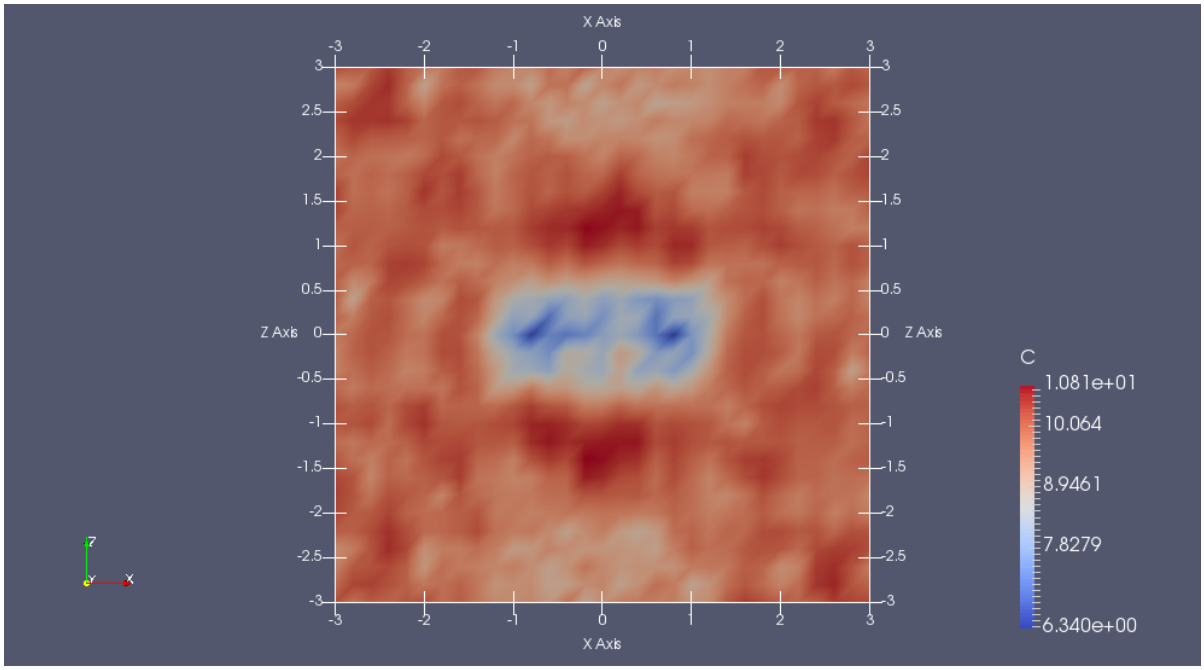

(b) Reconstructed Star along y-axis

Figure 5.13: Star along y-axis

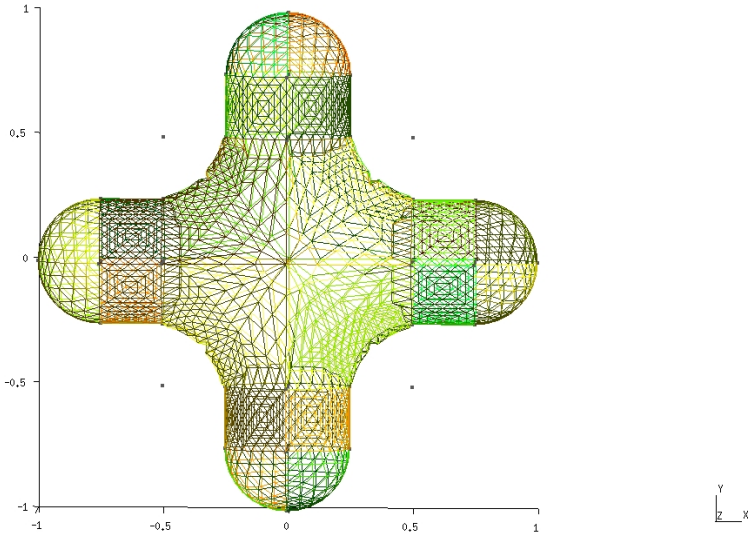

(a) Mesh of Star along z-axis

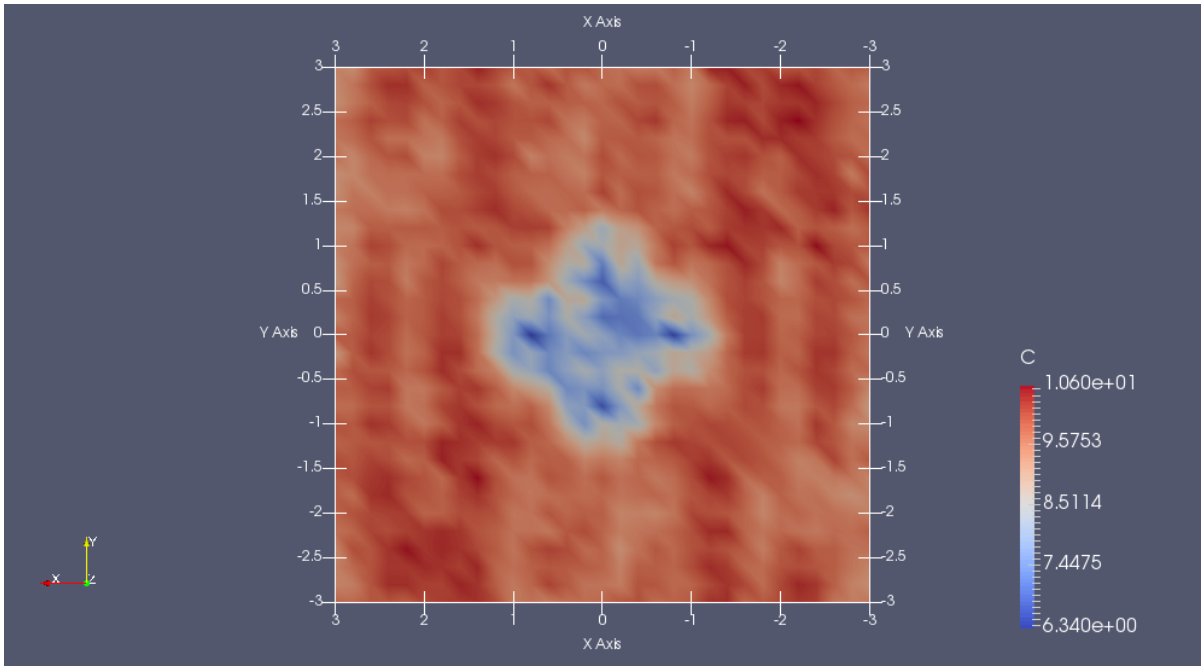

(b) Reconstructed ellipse along x-axis

Figure 5.14: Star along z-axis

Acknowledgement

The project was supported by grants from Naval Physical Oceanographic Laboratory, DRDO, India.

Bibliography

[1] A Regularized Sampling Method for Solving Three-Dimensional Inverse Scattering Problems, Colton, Giebermann, Monk, https://doi.org/10.1137/S1064827598340159

[2] Chandler-Wilde, S., Graham, I., Langdon, S., & Spence, E. (2012). Numerical-asymptotic boundary integral methods in high-frequency acoustic scattering. Acta Numerica, 21, 89-305. doi:10.1017/S0962492912000037

[3] On the numerical solution of the three-dimensional inverse obstacle scattering problem, Rainer Kress and Axel Zinn, http://www.sciencedirect.com/science/article/pii/037704279290162Q

[4] Inverse 3D acoustic and electromagnetic obstacle scattering by iterative adaptation, Haas, Martin and Rieger, https://doi.org/10.1007/BFb0105771

[5] An inverse problem for the three dimensional vector helmholtz equation for a perfectly conducting obstacle, Pierluigi Maponi and Luciano Misici and Francesco Zirilli, http://www.sciencedirect.com/science/article/pii/089812219190139U

[6] A simple method for solving inverse scattering problems in the resonance region, David Colton and Andreas Kirsch, http://stacks.iop.org/0266-5611/12/i=4/a=003

[7] Inverse Acoustic and Electromagnetic Scattering Theory,Colton, David, Kress, Rainer, No. 93 in Applied Mathematical Sciences, Springer-Verlag, New York, second ed., 1998.

[8] https://bempp.com/

[9] http://gmsh.info/

[10] https://www.paraview.org/

[11] https://www.gnu.org/software/octave/